energetic and entropic components which are sensitive to small differences in active site environments.

The total of thermodynamic data gathered for this system, and the ternary complex for the chicken species of DHFR reported in the previous paper in this series, are being used to examine the question of species specificity of trimethoprim for the bacterial species. The results of these studies are to be presented elsewhere.

Acknowledgment. Support from the NIH (Grant 37554) is gratefully acknowledged. C.L.B. is an Alfred P. Sloan Research Fellow. This research was supported in part by a grant from the Pittsburgh Supercomputing Center through the NIH Division of Research Resources Cooperative Agreement U41RR04154 and through a grant from the National Science Foundation Cooperative Agreement ASC-8500650.

Tunneling Dynamics in Isotopically Substituted Malonaldehyde. Comparison between Symmetric and Asymmetric Species

Enric Bosch, Miquel Moreno, and José M. Lluch*

Contribution from the Departament de Química, Universitat Autònoma de Barcelona, 08193 Bellaterra, Barcelona, Spain. *Received June 7, 1991*

Abstract: A theoretical study based on bidimensional model surfaces that retains the main features of the potential hypersurfaces has been performed in order to analyze the influence of primary and secondary effects on intramolecular proton transfer tunneling frequencies of malonaldehyde in the gas phase. To this aim, several isotopically substituted species have been considered. The tunneling frequency is calculated and compared for the different species. It is found that substitution of the transferring proton by deuterium or tritium greatly diminishes the tunneling whereas isotopic substitution of hydrogens not directly involved in the transfer has no appreciable effect when the symmetry of the double well is preserved. However, these secondary effects dramatically increase only by the introduction of a slight asymmetry in the double well potential by isotopic substitution. All these results agree with previous experimental data on isotopically substituted malonaldehyde species.

I. Introduction

The possibility of hydrogen tunneling in chemical reactions was recognized almost from the beginning of quantum theory.[1] Some of the most definite information about the part played by the tunnel effect in many processes comes from the study of isotope effects[1-16] on the rate of chemical processes.

Isotope effects can be classified as primary and secondary according to whether they involve isotopic substitution in a bond which is made or broken during reaction (i.e. primary) or in some other part of the reacting species (i.e. secondary). Primary deuterium and tritium isotope effects in proton-transfer reactions have been extensively used, but much less attention has been given to the secondary isotope effects.[4]

Experimentally, malonaldehyde (MA) is the prototype and most thoroughly investigated molecule for the study of proton transfer in polyatomic systems.[2,3,15] Regarding the isotope effects in this intramolecular reaction, the work of Baughcum et al.[2,3] is noteworthy since the primary and secondary effects are studied by the substitution of hydrogens by deuterium in different positions. An important point suggested by the authors is that a small asymmetry in the molecule induced by isotopic substitution could have an appreciable quenching effect when the transferring hydrogen has been substituted by a deuterium and only a partial effect when the transferring atom is a hydrogen.

From a theoretical point of view, a number of authors have dealt with the MA system.[17-24] However, to our knowledge, the isotopic substitution is only considered in the work of Shida et al.[22] where the primary isotope effect is evaluated.

The goal of this paper is to theoretically study the influence of the isotope effects on proton tunneling frequencies by analyzing several species of MA in the gas phase. Special attention will be

(1) Bell, R. P. *The Tunel Effect in Chemistry*; Chapman & Hall: London, 1980.
(2) Baughcum, S. L.; Duerst, R. W.; Rowe, W. F.; Smith, Z.; Wilson, E. B. *J. Am. Chem. Soc.* **1981**, *103*, 6296.
(3) Baughcum, S. L.; Smith, Z.; Wilson, E. B.; Duerst, R. W. *J. Am. Chem. Soc.* **1984**, *106*, 2260. Turner, P.; Baughcum, S. L.; Coy, S. L.; Smith, Z. *J. Am. Chem. Soc.* **1984**, *106*, 2265.
(4) Saunders, W. H., Jr. *J. Am. Chem. Soc.* **1985**, *107*, 164.
(5) Dormans, G. J. M.; Buck, H. M. *J. Am. Chem. Soc.* **1986**, *108*, 3253.
(6) Cha, Y.; Murray, C. J.; Klinman, J. P. *Science* **1989**, *243*, 1325. Grant, K. L.; Klinman, J. P. *Biochemistry* **1989**, *28*, 6597.
(7) Chantranupong, L.; Wildman, T. A. *J. Am. Chem. Soc.* **1990**, *112*, 4151.
(8) Wolfe, S.; Hoz, S.; Kim, C.; Yang, K. *J. Am. Chem. Soc.* **1990**, *112*, 4186.
(9) Amin, M.; Price, R. C.; Saunders, W. H., Jr. *J. Am. Chem. Soc.* **1990**, *112*, 4467.
(10) Redington, R. L. *J. Chem. Phys.* **1990**, *92*, 6447.
(11) Tucker, S. C.; Truhlar, D. G. *J. Am. Chem. Soc.* **1990**, *112*, 3338.
(12) Truong, T. N.; Truhlar, D. G. *J. Chem. Phys.* **1990**, *93*, 2125.
(13) Lu, D.-h.; Maurice, D.; Truhlar, D. G. *J. Am. Chem. Soc.* **1990**, *112*, 6206 and references 15-30 cited therein.
(14) Firth, D. W.; Barbara, P. F.; Trommdorsf, H. P. *Chem. Phys.* **1989**, *136*, 349.
(15) Seliskar, C. J.; Hoffman, R. E. *J. Mol. Spectrosc.* **1981**, *88*, 30; **1982**, *96*, 146.
(16) Swinney, T. C.; Kelley, D. F. *J. Phys. Chem.* **1991**, *95*, 2430.
(17) Fluder, E. M.; De la Vega, J. R. *J. Am. Chem. Soc.* **1978**, *100*, 5265.
(18) De la Vega, J. R. *Acc. Chem. Res.* **1982**, *15*, 185.
(19) Bicerano, J.; Schaefer, H. F., III; Miller, W. H. *J. Am. Chem. Soc.* **1983**, *105*, 2550.
(20) Carrington, T., Jr.; Miller, W. H. *J. Chem. Phys.* **1986**, *84*, 4364.
(21) Hutchinson, J. S. *J. Phys. Chem.* **1987**, *91*, 4495.
(22) Shida, N.; Barbara, P. F.; Almlöf, J. E. *J. Chem. Phys.* **1989**, *91*, 4061.
(23) Makri, N.; Miller, W. H. *J. Chem. Phys.* **1989**, *91*, 4026.
(24) Bosch, E.; Moreno, M.; Lluch, J. M.; Bertrán, J. *J. Chem. Phys.* **1990**, *93*, 5685.

0002-7863/92/1514-2072$03.00/0 © 1992 American Chemical Society

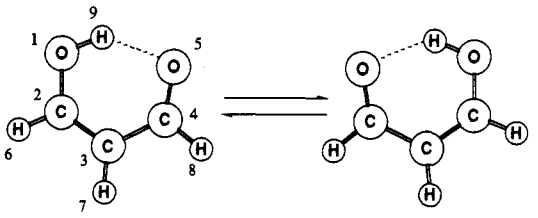

Figure 1. Intramolecular proton-transfer reaction in malonaldehyde. Numeration of atoms is used in the text to designate the isotopically substituted atoms.

paid to the secondary isotope effect in systems where the symmetry of the molecule is broken.

To designate isotopic species, we will show in parentheses the isotopic atoms which replace the normal ones at specified positions and a subscript will be used to indicate the atomic positions as shown in Figure 1.

The rest of the paper is structured as follows: Section II describes the calculational details. In sections III and IV tunneling in symmetrically and asymmetrically substituted isotopic species of malonaldehyde are respectively studied. Finally, section V gives the conclusions.

II. Calculational Details

The theoretical study of tunneling in polyatomic systems is difficult due to the increasing number of degrees of freedom to be considered. A very commonly used method to evaluate this quantum effect is to employ the intrinsic reaction coordinate (IRC)[25-29] as a monodimensional tunneling path.

For a transfer of a light atom between two heavy centers the IRC usually becomes too curved so that from a quantum point of view the tunneling dynamics does not follow the IRC allowing the tunneling path to cut the corner. In order to circumvent this problem the use of a linear path (LRP) has been suggested.[30,31]

An additional drawback arising from the reduction of the dimensionality is an incomplete introduction of the zero point energy (ZPE) correction.[24] On the other hand, a bidimensional representation of the potential energy surface based on the monodimensional IRC and LRP paths and including in some manner the ZPE correction seems to work well for this system.[24]

In the following, we will begin in subsection A by obtaining the ab initio reaction paths which are used in subsection B to build up the bidimensional surfaces. Then in subsection C the tunneling model used in this paper will be discussed.

A. Ab Initio Reaction Paths. Given that the isotopic substitution does not change the potential energy surface, the structure of the minima and transition state for proton transfer are the same for all the isotopic species of MA. The corresponding 3-21G ab initio structures are taken from our previous paper.[24] Conversely, IRC and LRP have to be re-evaluated for any different isotopic species using the same basis set.

For each isotopic species the IRC has been computed with the GAMESS[32] program by going downhill from the transition state to minima in mass-weighted Cartesian coordinates.[33,34] The unique mode with imaginary frequency determines the starting direction away from the transition state. Assuming the harmonic approximation, we chose the initial step size Δs that produced the appropriate energy lowering $f(\Delta s)^2/2$, where f is the negative force constant associated with the imaginary frequency. Then the IRC is followed taking successive very small steps in the direction of the negative gradient, which is equivalent to the Euler method. An initial energy lowering of 0.0005 hartree and then successive steps of $\Delta s = 0.0265$ amu$^{1/2}$·Å have been used for the proton-transfer reactions.

The LRP is defined as a straight line obtained by linear interpolation between the reactant and product in mass-weighted Cartesian coordinates. The origin of axes is always at the center of mass of the molecule, and the product axes system is orientated in precisely the correct manner with respect to that of the reactant that the requirements of the linear path not having any linear or angular momentum generated along it are fulfilled.[30]

B. Bidimensional Potential Energy Surfaces. In principle, in order to study the tunneling dynamics the exact quantum hamiltonian in the multidimensional hypersurface of the system should be diagonalized. However, the number of degrees of freedom involved in the MA system makes this calculation unattainable. To circumvent this problem we have fitted[24] a two-dimensional quartic polynomial approximation that retains the main features of the true multidimensional surface which are relevant in tunneling dynamics. This reduces the problem to the diagonalization of a bidimensional hamiltonian which can be performed using an appropriate basis set. In particular we have considered a potential used previously for the MA proton transfer by several authors[23,24,35-38]

$$V(x,y) = V_0(x) + \frac{1}{2}m\omega^2\left[y - \frac{g(x)}{m\omega^2}\right]^2 \quad (1)$$

where

$$V_0(x) = -ax^2 + bx^4 + dx^3 \quad (2)$$

$$g(x) = cx^2 \quad (3)$$

The polynomial used for $V_0(x)$ is a simple model for a double well potential. The parameter d vanishes when the double well is symmetric. The $g(x)$ formula is usually taken to represent a quadratic coupling. Finally we note that as mass-weighted Cartesian coordinates have been used a value of $m = 1$ has to be taken throughout all the calculations.

At this point it should be noted that in the multidimensional "real" surface, the ZPE of $3N - 6$ normal modes should be included whereas only two modes will be considered in the reduced bidimensional surface. In order to introduce the ZPE of the rest of the vibrational modes, an adiabatic correction has been adopted as explained in ref 24.

For a symmetric double well the four adjustable parameters a, b, c, and ω have been fitted in such a way that the lengths and the ZPE corrected energy barriers of IRC and LRP on the bidimensional surface coincide with the "true" values on the multidimensional surfaces obtained as described above.

For the other cases, as only a slight asymmetry is induced by isotopic substitution, the additional parameter d is adjusted so that the zero point energy difference between both wells is reproduced.

To clarify the relationship between the x and y variables and the real atomic displacements it has to be noted that two kinds of nuclear reorganization in going from reactants to products can be distinguished. Motions that strictly come from the geometric difference between reactant and product compose the first group. These motions lead from reactants to products through the shortest path. The x coordinate in the surfaces stands for this kind of motion. The displacement of the transferring H is the dominant component of this coordinate.

On the other hand, the second group of changes consist of distortions of the reactant in such a way that an approach to the geometry of the product is not provided but a path with lower energy barrier is allowed. The y coordinate denotes this kind of motion. In this way, the displacement along the y coordinate takes place only in order to facilitate the motion along the x coordinate, but the values of the y coordinate are identical for reactant and product. The more significant component to this coordinate is the stretching between the hydrogen-donor and hydrogen-acceptor oxygen.

We finally note that the parameter ω is the frequency of the bath represented by the y coordinate for all the points with $x = 0$ (this is the abscissa value at the transition state).

C. Tunneling Model. Assuming that our physical system has two vibrational states whose energies are close together and very different from those of all other states of the system, the problem is reduced to

(25) Truhlar, D. G.; Isaacson, A. D.; Garrett, B. C. In *Theory of Chemical Reaction Dynamics*; Baer, M., Ed.; CRC Press: Boca Raton, FL, 1985; Vol. IV, p 65.
(26) Truhlar, D. G.; Kupperman, A. *J. Am. Chem. Soc.* **1971**, *93*, 1840.
(27) Fukui, K. *J. Phys. Chem.* **1970**, *74*, 4161.
(28) Fukui, K. *Pure Appl. Chem.* **1982**, *54*, 1825.
(29) Miller, W. H.; Handy, N. C.; Adams, J. E. *J. Chem. Phys.* **1980**, *72*, 99.
(30) Miller, W. H.; Ruf, B. A.; Chang, Y. *J. Chem. Phys.* **1988**, *89*, 6298.
(31) Garrett, B. C.; Joseph, T.; Truong, T. N.; Truhlar, D. G. *Chem. Phys.* **1989**, *136*, 271.
(32) Dupuis, M.; Spangler, D.; Wendoloski, J. *National Resource for Computations in Chemistry Software Catalogue Program QG01* (Lawrence Berkeley Laboratory, US-DOE, 1980); Dupuis, M.; Spangler, D.; Wendoloski, J.; Schmidt, M. W.; Elbert, S. T. *GAMESS V. December 1989.*
(33) Schmidt, M. W.; Gordon, M. S.; Dupuis, M. *J. Am. Chem. Soc.* **1985**, *107*, 2585.
(34) Garrett, B. C.; Redmon, M. J.; Steckler, R.; Truhlar, D. G.; Baldridge, K. K.; Bartol, D.; Schmidt, M. W.; Gordon, M. S. *J. Phys. Chem.* **1988**, *92*, 1476.
(35) Makri, N.; Miller, W. H. *J. Chem. Phys.* **1987**, *86*, 1451.
(36) Makri, N.; Miller, W. H. *J. Chem. Phys.* **1987**, *87*, 5781.
(37) Walet, N. R.; Klein, A.; Dang, G. D. *J. Chem. Phys.* **1989**, *91*, 2848.
(38) Cukier, R. I.; Morillo, M. *J. Chem. Phys.* **1989**, *91*, 857; **1990**, *92*, 4833.

calculating the proton tunneling probabilities between a double well of finite barrier involving only these two states.

Let us initially consider that the barrier between wells is infinite. In this case there will be no tunneling so that two stationary states ψ_1 and ψ_2 with associated energy E_1 and E_2 appear, which correspond to the proton located in each side of the barrier.

When the barrier is finite a coupling W takes place between both wells so that ψ_1 and ψ_2 are no longer stationary states of the system. It can be easily shown[39] that the new stationary states ψ_+ and ψ_- have associated the following eigenvalues:

$$E_+ = \tfrac{1}{2}(E_1 + E_2) + \tfrac{1}{2}\sqrt{(E_1 - E_2)^2 + 4|W_{12}|^2} \quad (4)$$

$$E_- = \tfrac{1}{2}(E_1 + E_2) - \tfrac{1}{2}\sqrt{(E_1 - E_2)^2 + 4|W_{12}|^2} \quad (5)$$

where

$$W_{12} = \langle\psi_1|W|\psi_2\rangle \quad (6)$$

From the dynamic point of view, if initially the system is in the state ψ_1, at time t the wave function $\psi(t)$ is given by

$$\psi(t) = e^{i\Phi/2}\left[\left(\cos\frac{\theta}{2}\right)(e^{-iE_+t/\hbar})\psi_+ - \left(\sin\frac{\theta}{2}\right)(e^{-iE_-t/\hbar})\psi_-\right] \quad (7)$$

where θ is defined by

$$\tan\theta = \frac{2|W_{12}|}{E_1 - E_2} \quad (8)$$

and Φ is given by

$$W_{12} = |W_{12}|e^{i\Phi} \quad (9)$$

The probability amplitude P_{12} of finding the system at time t in the state ψ_2 can then be obtained:

$$P_{12}(t) = \frac{4|W_{12}|^2}{4|W_{12}|^2 + (E_1 - E_2)^2}\sin^2\left[\sqrt{4|W_{12}|^2 + (E_1 - E_2)^2}\frac{t}{2\hbar}\right] = (\sin^2\theta)\sin^2\left(\frac{E_+ - E_-}{2\hbar}t\right) \quad (10)$$

We observe that the probability oscillates over time with a frequency ν_t of $2(E_+ - E_-)/h$ between zero and the maximum value which is equal to $\sin^2\theta$. This value indicates the maximum fraction of the proton that leaks to the other well.

From eq 10 one obtains the tunneling frequency k:

$$k = \frac{2(E_+ - E_-)}{h}\sin^2\theta \quad (11)$$

As mentioned above the tunneling probability depends on the vibrational eigenvalues. In order to calculate them we use a basis set $\varphi_{i,n}$

$$\varphi_{i,n}(x,y) = \chi_i(x)\cdot\zeta_n(y - \lambda_i) \quad (12)$$

where χ_i are localized Gaussian functions[40]

$$\chi_i(s) = \left(\frac{\alpha}{\pi}\right)^{1/4}\exp\left[\frac{-\alpha}{2}(s - s_i)^2\right] \quad (13)$$

and $\zeta_n(y - \lambda_i)$ are shifted harmonic oscillator basis functions. The value of the shift λ_i is given by

$$\lambda_i = \frac{\langle\chi_i|f(x)|\chi_i\rangle}{m\omega^2} \quad (14)$$

Within this basis set we have constructed the matrix representation of the double well hamiltonian, whose elements have been reported by Makri and Miller.[35] Diagonalization of this matrix provides the energies (eigenvalues) and wave functions (eigenvectors) of the lowest states. Good convergence is found by using a 31 Gaussian functions and 4 harmonic oscillators basis set, which gives rise to 124 basis functions for the total system.

In order to evaluate the energies E_1 and E_2 of the states with infinite barrier, a similar calculation has to be done by considering separately the two sides of the double well. This calculation is not required when the double well is symmetric.

(39) Cohen-Tannoudji, C.; Diu, B.; Laloë, F. *Quantum Mechanics*; John Wiley & Sons: Paris, 1977.

(40) Hamilton, I. P.; Light, J. C. *J. Chem. Phys.* **1986**, *84*, 306.

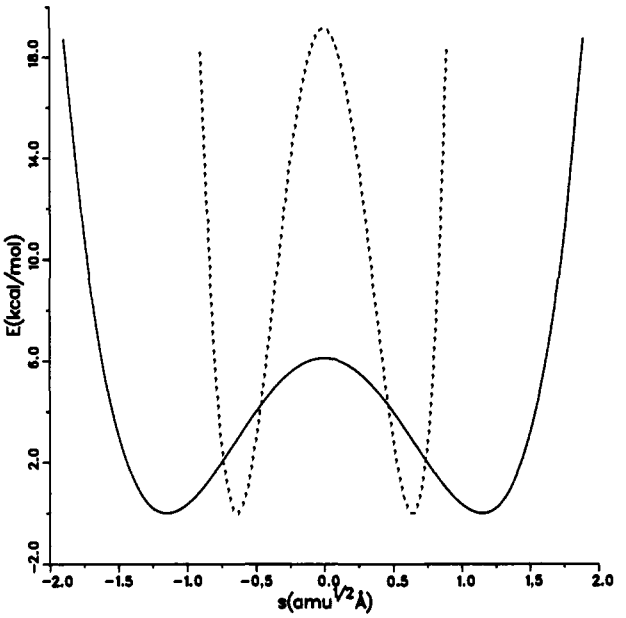

Figure 2. ZPE corrected intrinsic reaction coordinate (solid line) and linear reaction path (dashed line) energy profiles for the (D_9) isotopically substituted malonaldehyde. The parameter s stands for the arc length along each path.

Table I. Lengths and Energy Barriers for the Symmetrically Substituted Isotopic Systems

isotopic species	ΔS_{IRC}[a]	ΔS_{LRP}[a]	E_{IRC}[b]	E_{LRP}[b]
parent	2.08	0.97	5.31	18.34
(D_9)	2.29	1.28	6.11	19.15
(T_9)	2.45	1.52	6.43	19.46
(D_7)	2.09	0.97	5.31	18.34
(D_6,D_8)	2.10	0.98	5.30	18.33
(D_6,D_7,D_8)	2.09	0.98	5.31	18.34
(D_7,D_9)	2.29	1.28	6.12	19.15
(D_6,D_8,D_9)	2.30	1.28	6.11	19.14
(D_6,D_7,D_8,D_9)	2.29	1.29	6.12	19.15
(D_7,D_9,$^{18}O_1$,$^{18}O_5$)	2.38	1.29	6.11	19.14

[a] Total length in amu$^{1/2}$·Å. [b] Energy barrier in kcal·mol^{-1}.

III. Tunneling in Symmetrically Substituted Isotopic Species

In this section we will deal with the tunneling effects of malonaldehyde isotopic species where the symmetry of the double well parent molecule is preserved. According to the methodology previously presented, the IRC and LRP ab initio paths have been obtained for the different cases. As an example, the ZPE corrected IRC and LRP profiles for the (D_9) isotopically substituted MA have been depicted in Figure 2. The lengths and the ZPE corrected barriers for all the studied species are presented in Table I.

From the results presented in Table I some interesting points can be discussed.

As we are using mass-weighted Cartesian coordinates, when an isotope substitution affects an atom that moves along a given path, the path length will increase proportionally to the participation of the atom motion in the total length of the path. The LRP consists of motions strictly along the x coordinate. The transferring proton, atom number 9, is the only one clearly involved in this path, so an appreciable increment of the LRP length takes place when hydrogen 9 is substituted by deuterium or, more appreciably, by tritium.

Obviously, the transferring atom motion also takes place along the IRC so that the same length increment is observed along this path with deuterium and tritium substitution. However, the IRC implies motions not only along the x coordinate but also along the y coordinate. It has been shown[24] that the shortening of the proton acceptor and proton donor oxygen atoms distance has an important contribution to the IRC. Therefore, isotopic substitution of both oxygens by ^{18}O leads to an increment of the IRC length

Table II. Bidimensional Surface Adjustable Parameters for the Symmetrically Substituted Isotopic Species

isotopic species	a^a	b^b	c^c	ν^d
parent	44.8	94.3	0.94	682
(D_9)	29.7	36.2	0.53	676
(T_9)	22.3	19.4	0.38	670
(D_7)	44.7	94.1	0.93	676
(D_6,D_8)	44.4	93.2	0.92	671
(D_6,D_7,D_8)	44.5	93.1	0.93	678
(D_7,D_9)	29.8	36.2	0.54	675
(D_6,D_8,D_9)	29.6	35.8	0.53	668
(D_6,D_7,D_8,D_9)	29.6	35.8	0.53	673
(D_7,D_9,$^{18}O_1$,$^{18}O_5$)	29.4	35.4	0.50	638

[a] In kcal·mol^{-1}·Å^{-2}·amu^{-1}. [b] In kcal·mol^{-1}·Å^{-4}·amu^{-2}. [c] In mdyn·Å^{-2}. [d] In cm^{-1}.

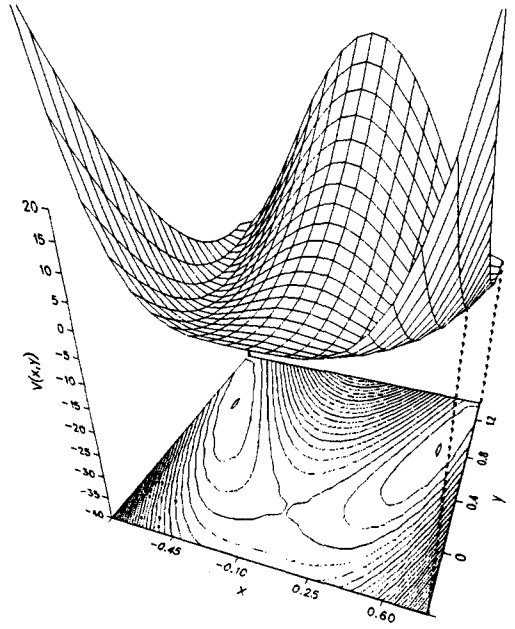

Figure 3. A three-dimensional perspective and contour plot of the bidimensional energy surface for the (D_9) isotopically substituted malonaldehyde. x and y coordinates are in amu$^{1/2}$·Å and the potential energy in kcal/mol.

whereas in this case the LRP remains almost unchanged.

Finally there are atoms that do not make any noticeable contribution to the path lengths so that an isotopic substitution of them does not affect the total length of the paths. As seen in Table I, hydrogens 6, 7, and 8 pertain to this kind of atom.

Regarding the energy barriers, for the IRC the difference between the isotopic species comes only from the different ZPE corrections. As this correction depends only on atoms that directly intervene in a bond that is formed or broken during the reaction, a higher barrier is obtained only when the transferring hydrogen 9 has been substituted by a heavier isotope. Finally, we note that as the same correction of the IRC is applied to the LRP, the barrier variations along this path follow the same trends as those of the IRC.

With the lengths and barriers presented in Table I we have fitted the parameters in eq 1–3 so that bidimensional analytic surfaces are readily obtained. The values of the adjusted parameters for the different symmetric species are shown in Table II. The frequencies ν presented in this table are related to ω in eq 1 by the usual formula

$$\omega = 2\pi\nu \tag{15}$$

For illustrative purposes Figure 3 depicts one of the bidimensional surfaces for the studied cases (the (D_9) species). As in the parent malonaldehyde molecule already studied,[24] the x coordinate coincides with the LRP direction which is mainly represented by the transferring proton motion. On the other hand, the y coordinate represents the modes that couple to the proton transfer along the IRC. As previously noted, the O–O stretching is the more significant component to this coordinate.

Table III. Splittings and Tunneling Frequencies[a] for the Symmetrically Substituted Isotopic Systems

isotopic species	$E_+ - E_-$[b]	k[c]
parent	8.20	4.92 (11)
(D_9)	0.30	1.80 (10)
(T_9)	0.03	1.80 (9)
(D_7)	7.90	4.74 (11)
(D_6,D_8)	7.94	4.76 (11)
(D_6,D_7,D_8)	7.93	4.75 (11)
(D_7,D_9)	0.29	1.74 (10)
(D_6,D_8,D_9)	0.29	1.74 (10)
(D_6,D_7,D_8,D_9)	0.29	1.74 (10)
(D_7,D_9,$^{18}O_1$,$^{18}O_5$)	0.26	1.56 (10)

[a] Power of 10 in parentheses. [b] Splitting in cm^{-1}. [c] Tunneling frequency in s^{-1}.

In the transition state the y direction is orthogonal to the IRC and the corresponding frequency has a value of ν. As seen in Table II, this frequency presents only small variations along all the studied isotopes with the exception of the (D_7,D_9,$^{18}O_1$,$^{18}O_5$) case where a lower frequency is obtained. This result agrees with our previous interpretation as the O–O stretching frequency will be lower when the mass of the atoms is increased. The value of this frequency in the transition state for the "true" parent malonaldehyde multidimensional surface of 674 cm^{-1} provides further agreement to that assignation.

For these symmetrical double well problems the energies of the "uncoupled" E_1 and E_2 states are the same and thus

$$E_+ - E_- = 2|W_{12}| \tag{16}$$

In this special case sin θ takes its maximum value of 1 and eq 10 reduces to

$$P_{12}(t) = \sin^2\left[\left(\frac{E_+ - E_-}{2\hbar}\right)t\right] \tag{17}$$

So in this case the tunneling frequency k coincides with the frequency ν_t with which the maximum leakage of the proton to the other well occurs.

Table III presents, for the different symmetric substituted isotopic species, the tunneling splitting ($E_+ - E_-$) and the tunneling frequency k. We observe that the isotopic substitution of the transferring proton (primary effect) leads to a dramatic diminution of the splitting and, consequently, of the tunneling frequency. In fact, when hydrogen 9 is substituted by deuterium the splitting reduces one order of magnitude whereas for the tritium species the reduction rises to an additional order of magnitude.

On the contrary, substitution of some of the nontransferring hydrogens by deuterium has only a very minor effect on the tunneling splitting as seen in Table III. Thus, the secondary isotopic effect is usually negligible, the splitting depending only on whether the transferring hydrogen has been deuterated. The only exception to this fact is found for the isotopically substituted oxygen species presented in the last row of Table III where a clearly lower splitting is obtained confirming the participation of oxygens in the proton transfer tunneling dynamics. We finally note that these results do not hold for the asymmetrically substituted isotopic species which will be considered in the next section.

Comparison of our results with experimental results for some of the studied species[3] shows that theoretical splittings are always clearly below the experimental values. However, the relative values between different isotopic species are consistent with experiment with the exception of the (D_6,D_8,D_9) species where the experimental splitting seems anomalously high.

IV. Tunneling in Asymmetrically Substituted Isotopic Species

In order to evaluate the effect of the breaking of the symmetry in the tunneling dynamics with isotopic substitution we have considered two species (D_6,D_7) and (D_6,D_7,D_9) which can be compared with the symmetric (D_6,D_8) and (D_6,D_8,D_9) species considered in the previous section.

Table IV. Lengths, Energy Barriers, and Double Well Asymmetry for the Asymmetrically Substituted Isotopic Systems

isotopic species	ΔS_{IRC}[a]	ΔS_{LRP}[a]	E_{IRC}[b]	E_{LRP}[b]	E_{ASYM}[b]
(D_6,D_7)	2.09	0.98	{5.36} {5.25}	{18.39} {18.29}	0.10
(D_6,D_7,D_9)	2.30	1.28	{6.17} {6.07}	{19.20} {19.10}	0.10

[a] Total length in amu$^{1/2}$·Å. [b] Energy in kcal·mol^{-1}.

Table V. Bidimensional Surface Adjustable Parameters for the Asymmetrically Substituted Isotopic Species

isotopic species	a[a]	b[b]	c[c]	ν[d]	d[e]
(D_6,D_7)	44.6	93.6	0.92	674	0.41
(D_6,D_7,D_9)	29.7	36.0	0.53	667	0.18

[a] In kcal·mol^{-1}·Å^{-2}·amu^{-1}. [b] In kcal·mol^{-1}·Å^{-4}·amu^{-2}. [c] In mdyn·Å^{-2}. [d] In cm^{-1}. [e] In kcal·mol^{-1}·Å^{-3}·amu$^{-3/2}$.

Table VI. Energy Differences and Tunneling Frequencies[a] for the Asymmetrically Substituted Isotopic Systems

isotopic species	$E_1 - E_2$[b]	$\sin^2\theta$	ν_t[c]	k[c]
(D_6,D_7)	24.9	0.081	1.56 (12)	1.30 (11)
(D_6,D_7,D_9)	28.4	0.00044	1.70 (12)	7.4 (8)

[a] Power of 10 in parentheses. [b] In cm^{-1}. [c] In s^{-1}.

Table IV presents the lengths and ZPE corrected barriers along the IRC and LRP paths for both asymmetrical species. The asymmetry of the double well is denoted in the last column of Table IV where the energy difference between both wells E_{ASYM} is calculated. Due to this slight asymmetry, two different barriers have to be given for both the IRC and LRP paths.

When comparing the data in Table IV with the same results for the symmetric (D_6,D_8) and (D_6,D_8,D_9) species presented in Table I, we note that the change of D_7 by D_8 does not produce any notorious variation in the calculated lengths and barriers so that the only difference comes from the small asymmetry character (0.1 kcal/mol) introduced.

With the lengths and barriers of Table IV we can now obtain analytical bidimensional surfaces by fitting the parameters in eq 1. Results are presented in Table V.

Results in Table V are again readily comparable to those of the corresponding symmetric species shown in Table II with the addition of the term d which now, given the asymmetry of the system, has a nonzero value.

In order to determine the vibrational levels of these asymmetric systems, (4) and (5) can be written in the form of a limited power series expansion in $|W_{12}|/(E_1 - E_2)$ up to a second order. The following expressions are obtained:

$$E_- = E_2 - \frac{|W_{12}|^2}{E_1 - E_2} \tag{18}$$

$$E_+ = E_1 + \frac{|W_{12}|^2}{E_1 - E_2} \tag{19}$$

where it has been assumed that $E_1 > E_2$.

Table VI gives the main parameters that characterize the tunneling dynamics of these systems. The last column in Table VI, which gives the tunneling frequency, can be readily compared with the same magnitude in Table IV for the corresponding symmetric species. This comparison clearly shows that now the purely secondary effect which presents the (D_6,D_7) species is already very important, the tunneling frequency having been clearly reduced. For the (D_6,D_7,D_9) species where both primary and secondary effects are present the quenching of tunneling by secondary isotopic effect is still magnified so that a very low value of k is obtained.

The reason for the difference between asymmetric and symmetric secondary effects can be analyzed by looking at the $\sin^2\theta$ and ν_t values whose product gives the tunneling frequency. It is clearly seen that the $\sin^2\theta$, which gives the fraction of the proton that tunnels to the other well, dramatically diminishes as compared with the value of unity for the symmetric cases. This effect cannot be totally compensated by the larger frequency ν_t, with which the maximum of probability density oscillates between both wells in the asymmetrical species.

Our results agree with a previous assumption done in order to interpret the microwave spectra of malonaldehyde and some isotopically substituted species.[3] In that work it was assumed that a small asymmetry in the potential could have a more appreciable quenching effect when the transferring proton is substituted by a deuterium. Similar symmetry-breaking effects to the ones reported here have also been previously predicted for other intramolecular proton transfer reactions.[41,42]

V. Conclusions

In this paper we have presented a theoretical study of the primary and secondary effects on proton tunneling dynamics of malonaldehyde. From a chemical point of view it has been shown that primary isotopic effects which take place by substitution of the transferring proton by deuterium or tritium leads to a considerable diminution of the tunneling frequency. On the other hand, substitution of hydrogens not directly involved in the proton transfer leads to a secondary effect which is negligible when the symmetry of the double well is preserved. However, if only a small asymmetry is introduced by isotopic substitution, the secondary effects dramatically increase. This quenching of tunneling by asymmetric isotopic substitution is still more important when the transferring proton is also substituted by a deuterium.

Finally it can be noted that the results presented here seem to confirm that our working bidimensional model retains the main features of the potential energy surfaces which are necessary in order to correctly evaluate the tunneling dynamics of the system and, therefore, it can be used to describe a variety of chemical problems.

(41) Kunze, K. L.; De la Vega, J. R. *J. Am. Chem. Soc.* **1984**, *106*, 6528.
(42) Hameka, H. F.; De la Vega, J. R. *J. Am. Chem. Soc.* **1984**, *106*, 7703.